Polymer 50 (2009) 117–124

Contents lists available at ScienceDirect

Polymer

journal homepage: www.elsevier.com/locate/polymer

Development of silk-like materials based on *Bombyx mori* and *Nephila clavipes* dragline silk fibroins

Mingying Yang, Junji Kawamura, Zhenghua Zhu, Kazuo Yamauchi, Tetsuo Asakura*

Department of Biotechnology, Tokyo University of Agriculture and Technology, Koganei, Tokyo 184-8588, Japan

ARTICLE INFO

Article history:
Received 1 May 2008
Received in revised form
28 September 2008
Accepted 4 October 2008
Available online 18 October 2008

Keywords:
Bombyx mori silk
Nephila clavipes dragline silk
Silk-like protein

ABSTRACT

In order to develop new silk-like materials in the form of fiber and non-woven nano-fiber, this study synthesized a new silk-like protein by selecting the sequence from the crystalline region of *Bombyx mori* silk fibroin, $(GAGSGA)_6$, to imitate the processing condition of the silk fibroin with the combination of the sequence YGGLGSQGAGRG, the hydrophilic motif of spider dragline silk which was considered as the origin of supercontraction of spider dragline silk (Yang Z, et al. J Am Chem Soc 2000;122: 9019–25). The CD pattern of the silk-like protein in hexafluoroacetone (HFA) indicates that it takes helical structure. The solid-state structures of the silk-like protein before and after methanol treatment were determined to be random coil and Silk II structure (mainly β-sheet structure), respectively, using ^{13}C CP/MAS NMR. The ^{13}C CP/MAS NMR spectra of the protein after methanol treatment in hydrated state showed that the random coil peaks from Ala Cβ and Ser Cβ carbons become sharper compared with the corresponding peaks in the dry state. The 2D-WISE spectra in the hydrated state also showed increase of the narrow components for these carbons. Thus, water molecules are relatively easy to access at the random coil regions of the protein. The fiber formation of the silk-like protein was possible with wet-spinning or electrospinning methods using HFA as dope solvent and methanol as coagulation solvent.

1. Introduction

The filaments produced by orb web spiders have been the focus of numerous recent investigations because they have a remarkable ability to spin a range of different silks, each optimized with respect to its specific biological function in nature [1–3]. Due to its size and the excellent mechanical properties, the dragline silk of the golden-orb weaver, *Nephila clavipes* (*N. clavipes*), has become the benchmark for the study of silk fibers [4,5]. Although spider dragline silk takes superior mechanical properties compared with silkworm silk, it has not been commercialized for biomedical applications, primarily due to the predatory nature of spiders and the relatively low levels of production of these silks. This technical hurdle seems to be addressed by turning to exploration of recombinant spider silk protein by bioengineering coupled with processing methods that can produce potential materials, such as fiber and nano-fiber prepared from bioengineered spider silks.

In order to design spider silk-like protein, accumulated information about structure–function relationships of spider silks is required. Besides the well-known superior mechanical properties, supercontraction of spider dragline silk has also been an another charming point that increasingly attracts the scientific concern. Supercontraction can be termed by that dragline silk fiber shrinks by 50% in length when it is exposed to water and results in rubber-like mechanical properties with an increase in elasticity and a decrease in strength and stiffness [6,7]. This supercontraction phenomenon can be basically ascribed to the primary sequences of spider dragline silk. Spider dragline silk is thought to be composed mainly of two proteins, spidroins I and II [4,5]. These proteins can be described as block copolymers with alternating polyalanine and glycine-rich blocks. It has been believed that the polyalanine domains form β-sheet crystals and contribute to the high strength and stiffness of fiber [8,9]. However, the glycine-rich regions were originally described to take amorphous [9], rubber-like [10], or 3_1-heical [11] forms. One highly conserved YGGLGSQGAGR sequence has been proposed to play a major role in the superconstraction process of the spider silk by Jelinski et al. [12]. They pointed out that Gly, Glu, Tyr, Ser, and Leu in the YGGLGSQGAGR sequence exhibit an increase in molecular motion when spider silk is in contact with water while the polyalanine, β-sheet region, displayed no change in dynamics [12,13]. Therefore, they proposed that the YGGLGSQGAGR sequence blocks in the major ampullate gland silk of the spider plays a major role in the interaction of the fibers with water and results in supercontraction. In addition, we synthesized this peptide, YGGLGSQGAGR, and found out that it is easily soluble in water and adopts random coil conformation [14].

* Corresponding author. Tel./fax: +81 42 383 7733.
E-mail address: asakura@cc.tuat.ac.jp (T. Asakura).

0032-3861/$ – see front matter © 2008 Elsevier Ltd. All rights reserved.
doi:10.1016/j.polymer.2008.10.008

On the other hand, appropriate spinning technologies capable of converting raw recombinant spider silk proteins into useful fibers or nano-fibers are required. In contrast to low level of production of spider silks, silkworm (*Bombyx mori*) cocoon silks are commercially available in large quantities. Therefore, several groups recently explored processing technologies by focusing on regeneration of fiber or nano-fiber from *B. mori* silk fibroin by using wet-spinning or electrospinning methods, which are benchmarks for the evaluation of the laboratory-based processing [15–19]. We have successfully produced regenerated fiber and nano-fiber by using hexafluoroacetone (HFA) as solvent for the preparation of silk dope and methanol as coagulation bath [15,16]. The information on processing of fiber and nano-fiber from *B. mori* silk fibroin might be a feedback to develop potential biomaterials from recombinant spider silks. However, the primary structure of *B. mori* silk fibroin is completely different from that of spider dragline silk. This implies that there is a possibility that the appropriate processing condition for *B. mori* silk might be not always optimal for spider silk. However, introduction of the sequence derived from *B. mori* silk fibroin into spider silk might increase a possibility in processing recombinant spider silk into fibers or nano-fibers. The primary structure of *B. mori* silk fibroin is mainly composed of repeated motifs, [GAGSGA]*n* and [GAGXGA]*n*, where X = Y or V. Motif [GAGSGA]*n* forms crystalline domains in *B. mori* silk fibroin, which has been considered to contribute to the strength of *B. mori* silk fiber [20]. It seems important to address whether silk-like protein composed of sequences from spider and *B. mori* silk fibroins can be processed in the forms of fiber and nano-fiber according to spinning condition of *B. mori* silk fibroin and also can regenerate similar structure of parental silk proteins.

This study designed a new silk-like material based on spider and *B. mori* silk fibroins. The crystalline region of *B. mori* silk fibroin, $(GAGSGA)_6$, was selected as functional sequence which is expected to be compatible to the spinning condition of *B. mori* silk fibroin. The sequence YGGLGSQGAGRG, the hydrophilic motif in the Gly-rich region of spider dragline silk which is considered as the origin of contraction of spider dragline silk, is selected as non-crystalline region in the recombinant silk. Thus, the primary structure of new silk-like protein was designed as $[(GAGSGA)_6$–YGGLGSQGAGRG]*n*. The solution structure of this new silk-like protein was characterized with CD method. The solid structure of silk-like protein in the dry and hydrated states was observed with ^{13}C CP/MAS and 2D WISE-NMR [21,22]. Formation of non-woven nano-fiber of this silk-like protein was performed with electrospinning method and also fiber formation with wet-spinning method.

2. Experimental part

2.1. Materials

Escherichia coli strain DH5α was used for propagation and construction of plasmids, and *E. coli* strain BL21(DE3)pLysS was used for production of proteins. Synthesized DNA fragments with phosphorylation were purchased from Sigma Genosys Ltd., Japan. Restriction enzymes and ligase were purchased from Takara Shuzo Ltd. Plasmid pUC118 and pET30a were obtained from Takara Shuzo and Novagen, respectively. Bacteria were grown in an enriched medium, and DNA manipulations and transformation were performed as described by Sambrook et al. [23]. DNA sequencing was performed on an ABI PRISM™ 377 Auto-sequencer according to the user's manual. *E. coli* cell density was measured at $\lambda = 600$ nm on a Hitachi U-3200 spectrophotometer in quartz cuvettes with a path length of 1 cm. Batch cultures were performed on MD-6C Fermentor (B.E.Marubishi Co.), with a 1.2 L vessel.

2.2. Gene construction

The oligonucleotide fragments encoding the crystalline domain of *B. mori* silk fibroin block and (Bc_3) and hydrophilic region from glycine-rich region of *N. clavipes* silk major ampullate spidroin 1(MaSP) are shown in Fig. 1a and b, respectively. Fig. 1c is the schematic drawing of gene construction. The oligonucleotide Bc_3 was firstly inserted into BamHI-digested pUC118 to construct pUC118-Bc_3. pUC118-Bc_6 was obtained by inserting fragment released from SpeI and NheI-digested pUC118-Bc_3 into NheI-digested pUC118-Bc_3 vector. The oligonucleotide MaSP was also inserted into BamHI-digested pUC118 and the fragment was released from pUC118-MaSP by degisting SpeI and Nhe I. Therefore, the monomer of silk-like protein Bc_6MaSP was constructed by ligating the fragment MaSP into SpeI-digested pUC118-Bc_6. The multimers of silk-like proteins Bc_6MaSP were obtained by using previously reported strategies involving the head-to-tail ligation and orientation for NheI and SpeI sites. Multimerized DNA fragments encoding these two recombinant proteins were inserted into the BamHI and HindIII-digested expression vector pET30a.

2.3. Protein expression and purification

Expression vectors containing the verified genetic constructs were transformed into the *E. coli* strain BL21(DE3)pLysS and subsequent cultures were grown in Luria–Bertain broth (TB) containing chloramphenicol (25 μl/ml) and kanamycin (25 μl/ml). Batch cultures of volumes of 1 L were allowed to grow at 37 °C to an optical density between 0.8 and 1.5, as determined by optical absorbance measured at 600 nm (OD_{600}). Protein expression, under control of a bacteriophage T7 promoter, was induced by addition of IPTG to a final concentration of 1 mM. Expression was continued for 1–2.5 h before harvest via centrifugation (8500 rpm, 40 min, 4 °C). The cells were collected and stored at −70 °C before purification. Protein expression and the level of expression were confirmed by Western blot analyses, where a T7-tag antibody–horseradish peroxidase conjugate was used for visualization. Purification was performed by using a nickel chelate affinity column which was charged with Ni^{2+} under native condition as previously reported. The eluted protein was dialyzed against distilled water for 3 days and then lyophilized.

2.4. ^{13}C solid state NMR measurement

Lyophilized Bc_6MaSP-4mer powders, and also the dried and hydrated samples after methanol/water treatment were used for ^{13}C solid state NMR experiments. The hydrated samples were prepared by adding deionized water, and then storing the wet sample at 4 °C for 24 h, finally, blotted with Kimwipes to remove excess water. The sample is packed in the rotor with epoxy in order to keep the sample with same moisture. About 40 mg of the sample contained in a cylindrical rotor with outer diameter of 4 mm. ^{13}C CP/MAS NMR spectra were acquired on a Chemagnetics CMX-400 spectrometer operating at 100 MHz, with a CP contact time of 3 ms, TPPM (two-pulse phase-modulated) decoupling [8], and magic angle spinning at 5 kHz. Spectra of 10,000–20,000 scans were accumulated over a spectral width of 80 kHz, with a recycle delay of 5 s. Chemical shifts were reported in parts per million relative to TMS as a reference. In order to further investigate the structure of silk-like protein in the hydrated state, WISE-NMR was performed according to the described by Holland et al. [21,22].

2.5. CD measurements

CD pattern of silk-like protein Bc_6MaSP-4mer dissolved in HFA was measured between 190 and 260 nm with a JASCO J-805

a crystalline region of *Bombyx mori* silk fibroin (Bc_3)

```
          Thr Ser Ala Gly Ser Gly Ala Gly Ala Gly Ser Gly Ala Gly Ala Gly Ser Gly Ala Gly Ala Ser
5' GA TCC ACT AGT GCT GGC TCC GGT GCC GGC GCG GGG AGC GGG GCA GGC GCA GGT TCT GGT GCA GGT GCT AGC G 3'
    3' G TGA TCA CGA CCG AGG CCA CGG CCG CGC CCC TCG CCC  CGT CCG CGT CCA AGA CCA CGT CCA CGA TCG CCT AG 5'
BamH I Spe I                                                                    Nhe I  Bam HI
```

b Hydrophilic region from glycine-rich region of *Nephila clavipes* silk major ampullate spidroin 1 (MaSP)

```
          Thr Ser Tyr Gly Gly Leu Gly Ser Gln Gly Ala Gly Arg Ala Ser
5' GA TCC ACT AGT TCT GGT GGC CTG GGC AGC CAG GGT GCG GGT CGT GCT AGC G 3'
    3' G TGA TCA AGA CCA CCG GAC CCT TCG GTC  CCA CGC CCA GCA CGA TCG CCT AG 5'
BamH I Spe I                                                  Nhe I  Bam HI
```

c Gene contruction of Bc_6MaSP-monomer

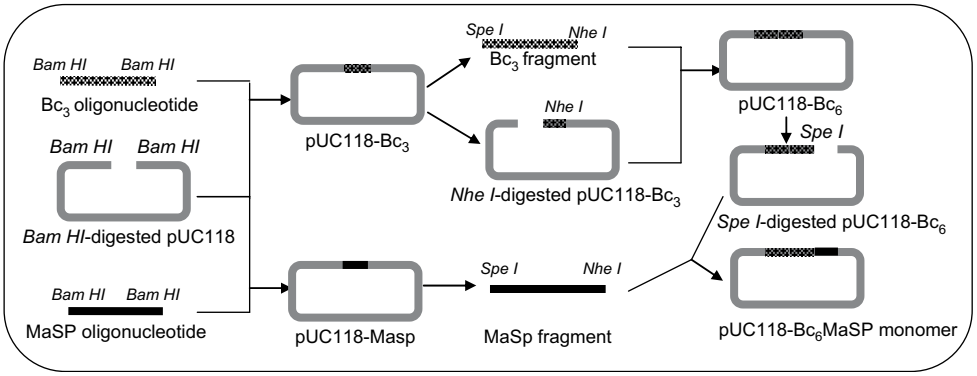

Fig. 1. The oligonucleotide sequence for silk-like protein Bc_6MaSP. (a) DNA sequence of crystalline region of *Bombyx mori* silk fibroin (BC_3). (b) DNA sequence of hydrophilic region from glycine from glycine-rich region of *Nephila clavipes* silk major ampullate spidroin 1(MaSP). (c) Schematic drawing of gene construction.

spectropolarimeter. The measurement was made at room temperature using a quartz cell with path length of 0.1 mm. The reported CD pattern represents an average of four consecutive scans, measured at 1 nm a resolution. The instrument was continuously flushed with dry nitrogen gas. The molar ellipticity $[\theta]_M$ values are determined by taking into account the molecular weight of 391 kDa with amino acid residues of 5263, reported for *B. mori* fibroin protein.

2.6. Differential scanning calorimetry measurement

DSC measurements were performed on a Rigaku Thermoflex (DSC8230D) (Rigaku Denki Co. Ltd., Japan) in the range of 30–350 °C, at the uniform heating rate of 10 °C/min. The sample weight and DSC range were about 5.4 mg and 2 mcal/s, respectively. An open aluminum pan was swept with nitrogen gas during the course of the heating process.

2.7. Electrospinning of silk-like protein

We reported previously the preparation of non-woven silk fibroin fibers from the HFA solutions of *B. mori* silk fibroin using electrospinning method [16]. The preparation method for silk-like proteins in this paper is essentially the same as the previous one: The silk-like proteins were dissolved in HFA and the optimal concentrations were determined as 10% by weight. In the electrospinning process, a high electric potential was applied to a droplet of silk solution at the tip (0.45 mm in internal diameter) of a plastic capillary. The electrospun fiber was collected on the mesh which was placed at a distance of 10 cm from the tip of the plastic capillary. Here, aluminum sheet was used as mesh. A voltage of 20 kV was applied to the wire in the capillary by a high voltage power supply to inject the silk solution on the aluminum sheet.

2.8. Fiber formation

Silk dope solution at concentration of 10% (W/W) was prepared by dissolving silk proteins in HFA solution. The silk solutions were loaded on a 1 ml syringe and extruded at room temperature with moderate force through internal 0.45 mm diameter hypodermic needle through an air gap of 10 mm. Methanol was used as coagulation bath. Attempts on post-treatment were made to soak fiber in the water at room temperature (water treatment) and to heat fiber in auto-cleaver at 100 °C, in 30 min (steam-annealing treatment) before drying in air.

2.9. SEM observation

Scanning electron microscope (KEYENCE VE-7800, Japan) was used to measure diameters and distribution of diameters of fibers prepared from electrospinning and wet-spinning. The distribution of fiber diameter for the non-woven fibers was sampled from 100 positions of fiber crossing in the SEM pictures.

3. Results and discussion

3.1. Gene construction and protein expression

Fig. 1a and b shows the oligonucleotide sequences encoding crystalline region of *B. mori* silk fibroin (Bc_3) and hydrophilic region from glycine-rich region of *N. clavipes* silk major ampullate spidroin 1(MaSP), respectively. Electrophoresis of the SpeI and NheI-digested recombinant cloning vectors, pUC118-linker-Bc_6MaSP-multimer against PCR markers confirmed genetic construction of monomer, dimer and tetramer, respectively, as shown in Fig. 2. Protein expression was performed by a commercially available expression vector pET30a, which contains $[His]_6$ sequence at the N-terminus and C-terminus of the recombinant protein for purification by immobilized metal affinity chromatography. Therefore,

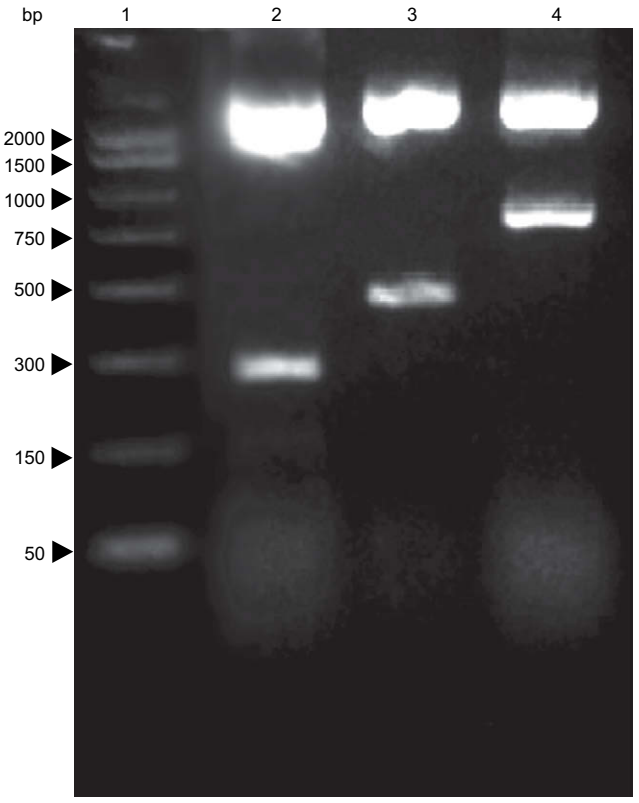

Fig. 2. SpeI and Nhe I digestion analysis of multimerized cloning vectors of Bc_6MaSP-4mer, Lane 1, PCR markers; lane 2, pUC118-monomer; lane 3, pUC118- dimer and lane 4, pUC118-tetramer.

purified pUC118-Bc_6MaSP-4mer DNA fragments were inserted into pET30a between BamHI and HindIII restriction sites, flanked by N- and C-terminal extensions of 53 and 19 amino acids, respectively. *E. coli* strain BL21(DE3)pLysS was used as the protein expression host. The pET30a-multimers were transformed into BL21(DE3)-pLysS and the encoded proteins were expressed upon induction of IPTG. Fig. 3a shows the Western blotting results by transferring the proteins from SDS-polyacrylamide gel, confirming the presence of the desired engineered proteins due to the appearance of band at about 30 kDa against positive control. Protein expressed from the pET30a vector was purified from the Ni-NTA affinity chromatography due to the $[His]_6$ sequence position at N-and C-termini. Fig. 3b shows the SDS-PAGE gel stained with Coomassie Blue R-250 for Bc_6MaSP-4mer. The molecular weight of Bc_6MaSP-4mer containing His-tags at N- and C-termini was estimated to be about 30 kDa against molecular weight mark, consistent with the predicted composition based on the translation of the coding sequence. After purification, the final yields were approximately 30 mg/L for Bc_6MaSP-4mer. For the structure analysis, His-tags at N- and C-termini were removed and the molecule weight is conformed in Fig. 3b.

3.2. CD analysis

To investigate the effect of introduction of hydrophilic sequence, YGGLGSQGAGR into the structure of *B. mori* silk fibroin, and to determine the effect of solvent HFA on the secondary structure of the protein in solution, Bc_6MaSP-4mer was characterized at room temperature. Fig. 4 shows the CD spectrum of silk-like protein Bc_6MaSP-4mer with the concentration of approximately 100 mM in HFA. The CD spectrum shows that the structure of silk-like protein Bc_6MaSP-4mer is predominantly helical due to the presence of double minima at ~206 and ~222 nm and a positive band at ~198 nm which are associated with helical structure. This pattern is similar to the CD patterns of Bc_5, $(GAGSGA)_5$ and *B. mori* silk fibroin dissolved in HFA, or spider silk in HFIP [24,25], indicating that silk-like protein Bc_6MaSP-4mer dissolved in HFA solvent can take similar secondary conformation to those of parental proteins, *B. mori* or spider silks. This implies that it is feasible to use HFA as reasonable solvent to prepare silk dope for generation of nano-fiber or fiber.

3.3. NMR analysis

Fig. 5 shows the ^{13}C CP/MAS NMR spectra of silk-like protein, Bc_6MaSP-4mer after dialysis followed by lyophilization (solid line) and 90% methanol/water treatment (dotted line) in order to investigate the effect of YGGLGSQGAGR on the structure of

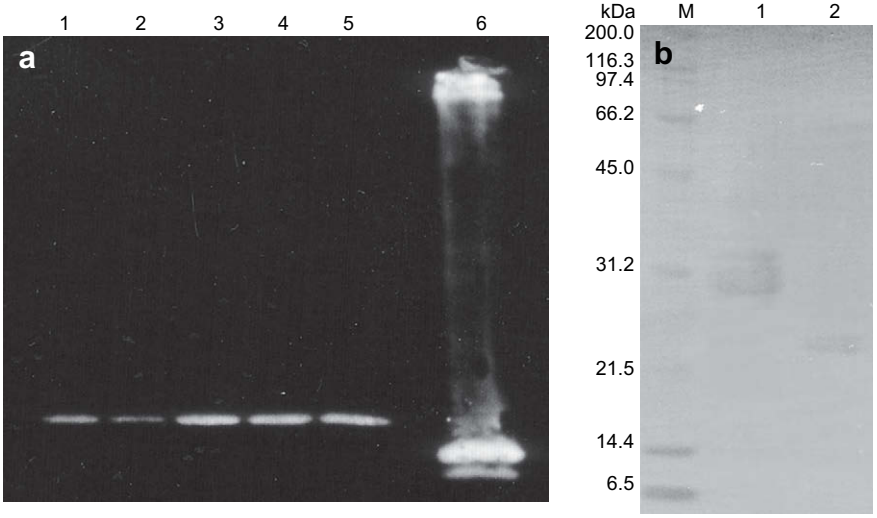

Fig. 3. (a) Western blottings of the successful construction and analysis of the expression level of Bc_6MaSP-4mer at different induction times. Lanes from 1 to 5 are cultured solution 0.5, 1, 1.5, 2 and 2.5 h after expression induced by IPTG addition, respectively. Lane 6 is SLP for positive control. (b) SDS-PAGE result of Bc_6MaSP-4mer containing His-tags stained with Coomassie Blue R-250. M: molecular weight marker (Bio-Rad). (c) SDS-PAGE result of Bc_6MaSP-4mer stained with Coomassie Blue R-250. M: molecular weight marker (Bio-Rad).

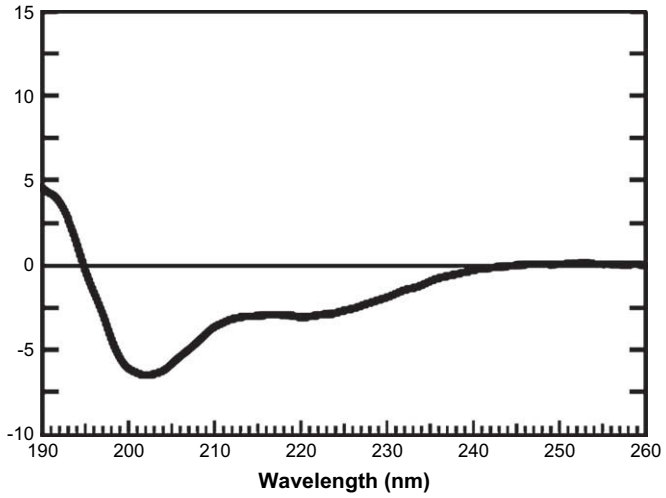

Fig. 4. CD spectrum of silk-like proteins Bc_6MaSP-4mer dissolved in solvent HFA·hydrate with 100 mM concentration.

$(GAGSGA)_6$. Dialysis and 90% methanol/water treatments were attempted to simulate the structure of silk-like protein Bc_6MaSP-4mer before and after spinning, respectively. Silk-like protein Bc_6MaSP-4mer adopts predominantly random coil conformation as judged from the main peak observed at 16.6 ppm (Ala Cβ) and 52.0 ppm (Ala Cα) after dialysis. By 90% methanol/water treatment, the main peak of Ala Cβ shifted to 22.2 ppm, Ala Cα to 49.0 ppm, and two distinctive peaks of Ala C═O and Gly C═O were observed clearly at 172.0 ppm and 169.1 ppm, respectively. This indicates that Bc_6MaSP-4mer takes Silk II structure [26]. Even in the case of Silk II structure of *B. mori* silk fibroin, the shoulder peaks of Ala Cβ at 16.6 ppm still remain, which indicate the presence of distorted β-turn structure [15]. Thus, Bc_6MaSP-4mer takes a similar structure as the parental protein *B. mori* silk fibroin in spite of the presence of YGGLGSQGAGR in the protein. This implies that it is possible to produce fiber or nano-fiber from this silk-like protein Bc_6MaSP-4mer by using the same processing methods to that of *B. mori* silk fibroin.

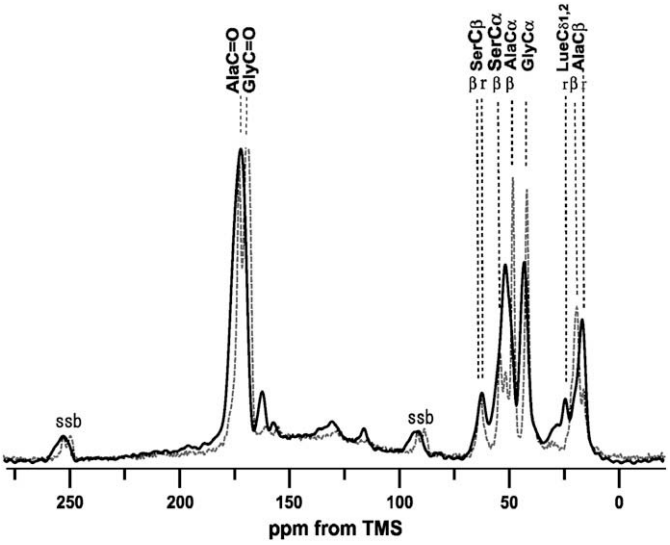

Fig. 5. ^{13}C CP/MAS NMR spectra of silk-like protein Bc_6MaSP-4mer and 90% methanol/water treatment. Solid line (—) is the spectrum of after dialysis followed by lyophilization. Dotted line (……) is the spectrum of silk-like protein Bc_6MaSP-4mer after 90% methanol/water treatment.

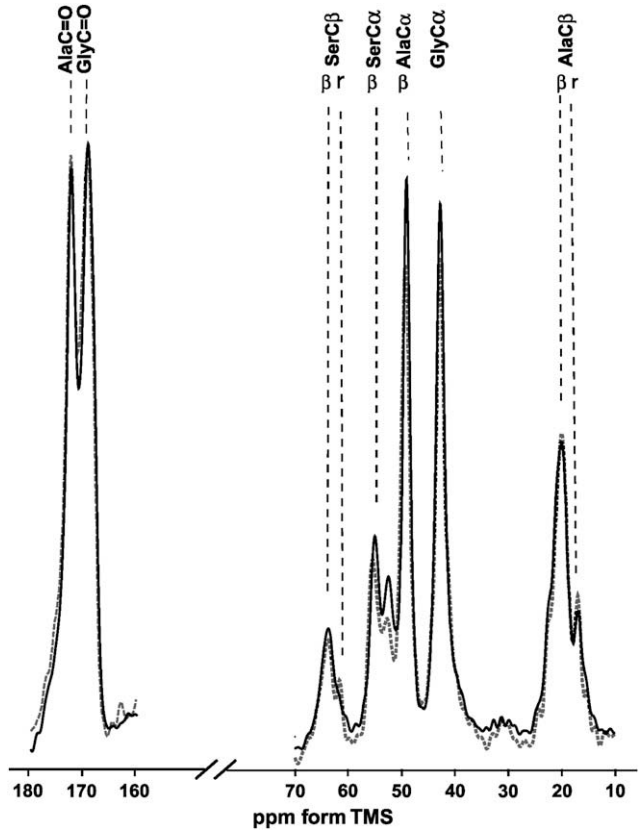

Fig. 6. ^{13}C CP/MAS NMR spectra of the silk-like protein Bc_6MaSP-4mer in the dry and the water wetted state. Dotted line (……) is the spectrum of the dry silk-like protein. Solid line (—) is the spectrum of hydrated silk-like protein.

The structure of Bc_6MaSP-4mer in dry (dotted line) and hydration (solid line) states was also compared with each other using ^{13}C CP/MAS NMR as shown in Fig. 6. The random coil peaks from Ala Cβ and Ser Cβ carbons become sharper compared with the corresponding peaks in the dry state. The peaks of Gly Cα, Ser Cα and Ser Cβ carbons decrease in the intensity significantly by hydration, indicating an increase in chain motion caused by the presence of

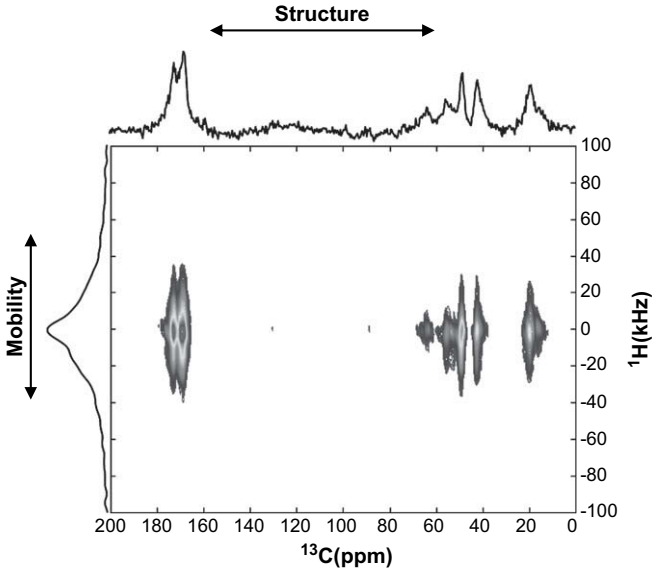

Fig. 7. 2D-WISE-NMR spectrum of silk-like protein Bc_6MaSP-4mer in the hydrate state.

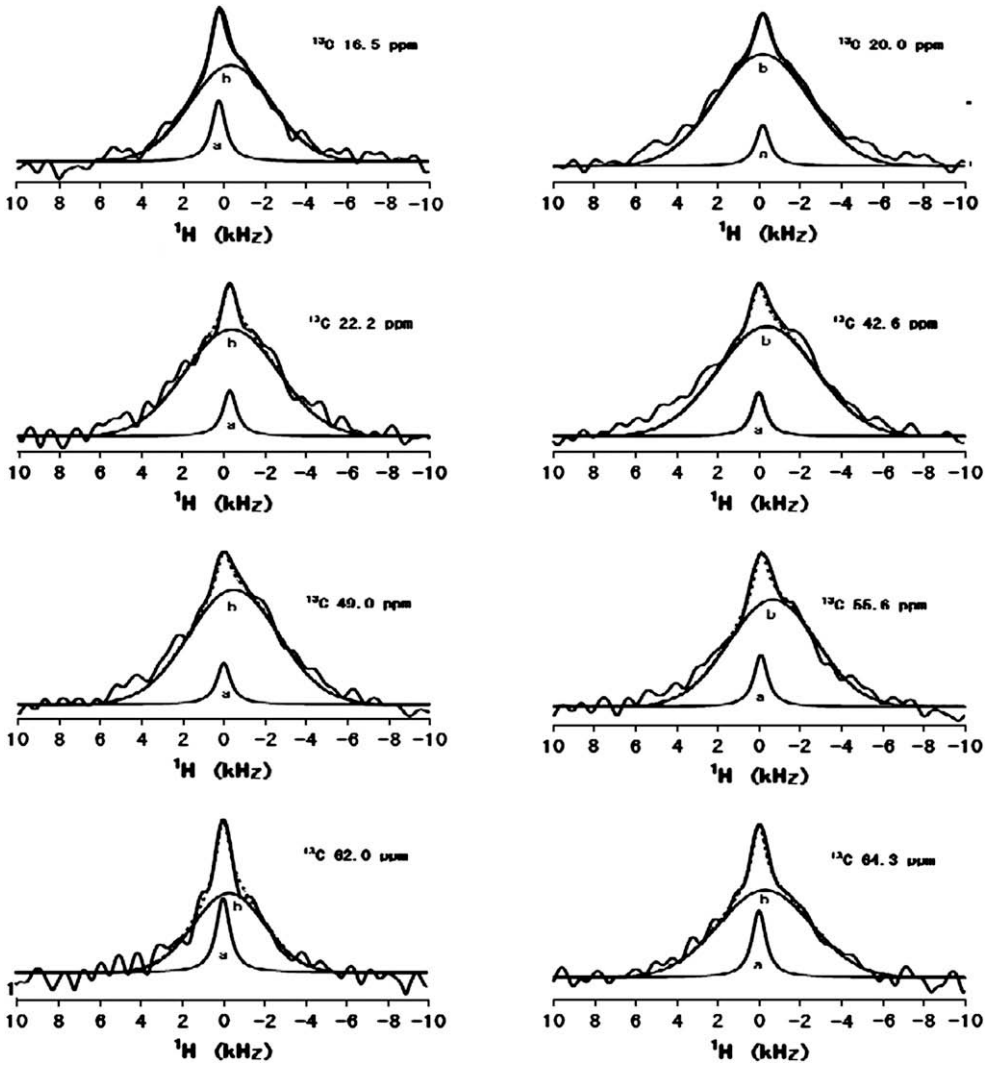

Fig. 8. ^{1}H slices corresponding to ^{13}C chemical shifts in the WISE spectrum of hydrated Bc_6MaSP-4mer (Fig. 7). The deconvoluted spectra are also shown: narrow component (a) and broad component (b). The super-imposed spectra, (a) plus (b), are shown as dotted lines.

water. The Ala Cα peak also decreases, but this region is overlapped with the Cα peaks of other residues in YGGLGSQGAGR. Therefore, the discussion of Ala residue seems better for the Ala Cβ peak.

The 2D-WISE-NMR contour spectrum of the hydrated silk-like protein is depicted in Fig. 7. The ^{1}H slice spectra for the broad and narrow components are summarized in Fig. 8 together with the deconvoluted spectra. The peaks of Ala Cβ carbon at 20.0 ppm and 22.2 ppm can be assigned to β-sheet structure clearly, and ^{1}H width of these two peaks are broad, about 53.2–56.8 kHz. The 2D-WISE spectra in the hydrated state also showed increase of the narrow components for Ala Cβ and Ser Cβ carbons. Thus, water molecules are relatively easy to access at the random coil regions of the protein. Especially, the ^{1}H slice of Ser Cβ carbon displays a small narrow component in the ^{1}H resonance at 8.1 kHz with fraction of 21% at 62.0 ppm and 14% at 64.3 ppm. The final results after simulation are summarized in Table 1. Thus, the Ser side chain is mobile in the hydrated state although it seems difficult to discuss the increase in motion quantitatively. There are still Ser residues which contribute to maintain Silk II structure through hydrogen bonding formation among backbone chains. Previous studies proposed that the peptide YGGLGSQGAGR in hydrated state takes random coil conformation and easy to access to water molecules [14]. Because of small peaks from Tyr, Leu and Arg residues and overlapped peaks of Gly, Ala and Ser residues in the sequence, YGGLGSQGAGR, it is difficult to point out clearly in the 2D-WISE spectra.

3.4. Electrospinning of silk-like protein

In order to process Bc_6MaSP-4mer, non-woven fiber was prepared from the HFA solutions using electrospinning method

Table 1
2D-WISE-NMR chemical shifts of hydrated B_{c6}MaSP-4mer. The assignment of the local conformations along with the fraction of broad and narrow components are also listed.

Carbon in amino acid	^{13}C chemical shift (ppm)	Assignment	Broad component	Narrow component
Ala Cβ	16.6	Random coil	46.5 kHz (86%)	8.1 kHz (14%)
	20.0	β-Sheet	53.2 kHz (92%)	8.1 kHz (8%)
	22.2	β-Sheet	53.2 kHz (91%)	8.1 kHz (9%)
Ala Cα	49.0	β-Sheet Random coil	53.1 kHz (92%)	8.1 kHz (8%)
Gly Cα	42.6	β-Sheet Random coil	56.8 kHz (92%)	8.1 kHz (8%)
Ser Cβ	62.0	Random coil	40.7 kHz (79%)	8.1 kHz (21%)
	64.3	β-Sheet	53.2 kHz (84%)	8.1 kHz (16%)
Ser Cα	55.6	β-Sheet Random coil	50.3 kHz (90%)	8.1 kHz (10%)

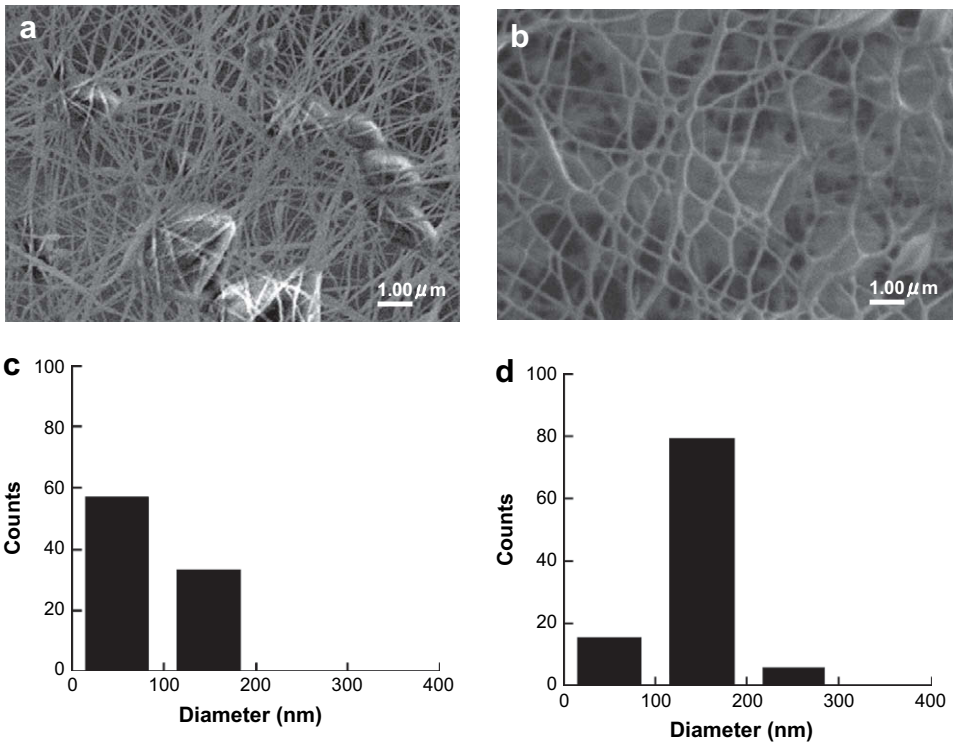

Fig. 9. Scanning electron micrograph of (a) non-woven fibers prepared from the silk-like protein Bc_6MaSP-4mer dissolved in solvent HFA·hydrate; (b) after methanol steam treatment; (c), (d) distribution of the diameter of fiber corresponding to (a), (b), respectively.

previously reported [16]. Fig. 9a and b shows the SEM morphology of the non-woven fibers spun from the HFA solutions of Bc_3MaSP-4mer with the concentrations of 10% and after methanol steam treatment, respectively. The long fiber could be prepared with silk-like protein Bc_6MaSP-4mer (Fig. 9a). After methanol steam treatment, the secondary structure changes to β-sheet form. The fine fibers aggregate to form thick fibers by network formation. Actually, the fiber diameter before steam treatment was averaged to be

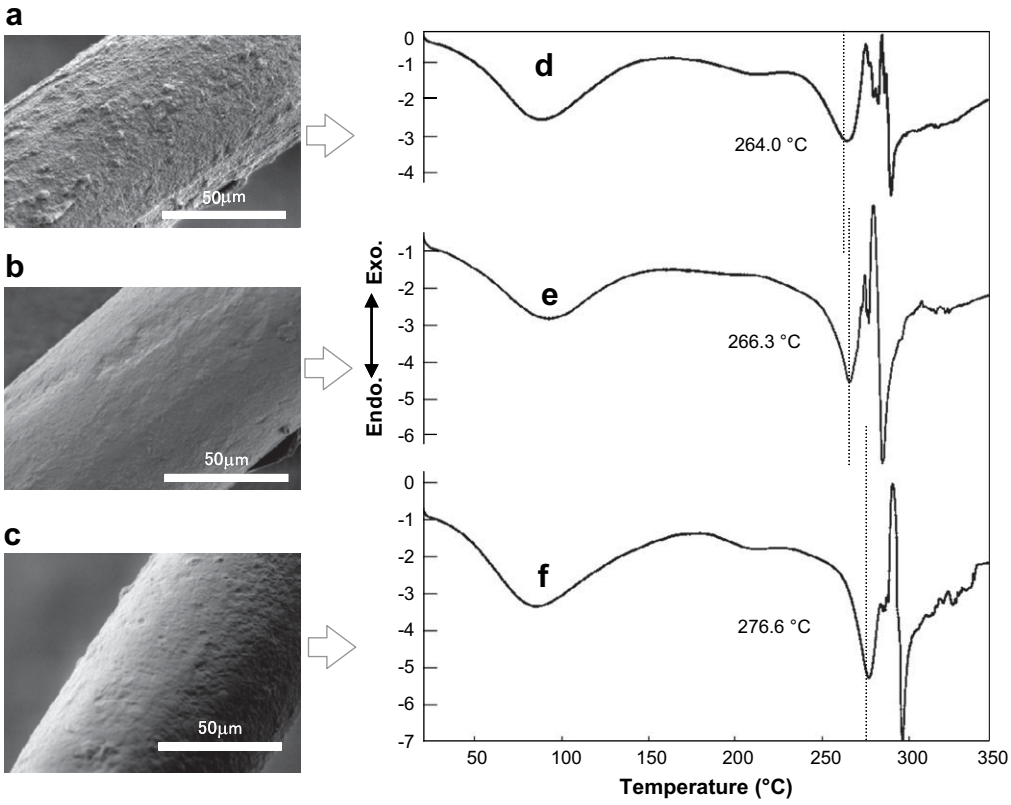

Fig. 10. Scanning electron micrograph of (a) as-spun fibers prepared from the silk-like protein Bc_6MaSP-4mer dissolved in solvent HFA·hydrate; (b) after water treatment; (c) after steam-annealing treatment; (d), (e), (f) DCS curves of corresponding to (a), (b), (c), respectively.

about 100 nm (Fig. 9c), but the mean fiber diameter increased to about 137 nm after methanol steam treatment (Fig. 9d). This indicates that silk-like protein composed of both sequences from spider and *B. mori* silk fibroins can be processed into nano-fiber according to spinning conditions of *B. mori* silk fibroin.

3.5. Fiber formation of silk-like protein

In order to use Bc_6MaSP-4mer, it is required to spin this protein into fiber. Spinning of Bc_6MaSP-4mer was performed by extruding the silk solution prepared from the HFA into coagulant methanol as shown in Fig. 10a. The diameter of the fiber is estimated as approximately 50 μm. As-spun fibers produced from silk-like protein Bc_6MaSP-4mer were birefringent, but brittle after drying. Post-treatment was then performed by soaking the fibers into water (water treatment) or by heating the fibers in autoclave at 100 °C for 30 min (steam-annealing treatment). The SEM pictures in Fig. 10b and c shows that the surface of the fiber tends to become smooth after water treatment and steam-annealing treatment. This might be due to increase of β-sheet crystallinity of fiber after post-treatment. DSC experiment was performed to prove this assumption. Fig. 10d–f shows DSC curves of fibers with and without post-treatment. The DSC curves displayed two endothermic peaks, one at around 70 °C is due to loss of water, and another is at 264 °C (as-spun), 266.3 °C (water treatment), and 276.6 °C (steam-annealing treatment), respectively, which are attributed to the thermal decomposition of fibers. After steam-annealing treatment, the DSC curve of the silk fiber showed a remarkable shift of the decomposition temperature by 12.6 °C compared with that of as-spun fiber. This indicated that the crystalline of fiber tends to increase after post-treatment. However, the thermal decomposition of the fibers, 276.6 °C, is lower than that of well-oriented *B. mori* silk fibers above 300 °C [27]. This implies that the crystallinity of fiber prepared from Bc_6MaSP-4mer is lower to that of native *B. mori* fiber from viewpoint of thermal character. This might be attributed to the introduction of hydrophilic sequence, YGGLGSQGAGR that decreases the crystallinity or due to the post-treatment that is not effective for increase in the crystallinity.

4. Conclusion

A new silk-like protein was constructed by combining the sequence YGGLGSQGAGRG, the hydrophilic motif of spider dragline silk which was considered as the origin of supercontraction of spider dragline silk [12] and the sequence, $(GAGSGA)_6$, the crystalline region of *B. mori* silk fibroin. By referring to the processing technologies performed on electrospinning and wet spinning of *B. mori* silk fibroin, nano-fiber by electrospinning and fiber by wet spinning of silk-like protein were formed. However, it is necessary to prepare well-ordered fiber of this silk-like protein with high molecular weight to discuss the supercontraction property clearly. The design, production and processing of silk-like materials with hydrophilic character coupled with structure determination provide a potentially power tool for studying the relationship between sequence and function, and the development of potentially useful materials.

Acknowledgements

TA acknowledges the support of Grant-in-Aid for Scientific Research from the Ministry of Education, Science, Culture and Sports of Japan (18105007).

References

[1] O'Brien JP, Fahnestock SR, Termonia Y, Gardner KH. Adv Mater 1998;10:1185–95.
[2] Gosline JM, Guerette PA, Ortlepp CS, Savage KN. J Exp Biol 1999;202:3295–303.
[3] Vollrath F, Knight DP. Nature 2001;410:541–8.
[4] Xu M, Lewis RV. Proc Natl Acad Sci U S A 1990;87:7120–4.
[5] Hinman MB, Lewis RV. J Biol Chem 1992;267:19320–4.
[6] Work RW. Trans Am Microsc Soc 1977;100:1.
[7] Work RW. J Exp Biol 1977;118:379.
[8] Simmons AH, Ray ED, Jelinski LW. Macromolecules 1994;27:5235–337.
[9] Grubb DT, Jelinski LW. Macromolecules 1997;30:2860–7.
[10] Michal CA, Jelinski LW. J Biolmol NMR 1998;12:231–41.
[11] Kümmerlen J, van Beek JD, Vollrath F, Meier BH. Macromolecules 1996;29:2920–8.
[12] Yang Z, Liivak O, Seidel A, Laverda G, Zax DB, Jelinski LW. J Am Chem Soc 2000;122:9019–25.
[13] Michal CA, Jelinski LW. J Biomol NMR 1998;12:231–41.
[14] Asakura T, Yang M, Kawase T. Polym J 2004;36:999–1003.
[15] Yao JM, Masuda H, Zhao CH, Asakura T. Macromolecules 2002;35:6–9.
[16] Ohgo K, Zhao C, Kobayashi M, Asakura T. Polymer 2003;44:841–6.
[17] Seidel A, Liivak O, Jelinske LW. Macromolecules 1998;31:6733–6.
[18] Seidel A, Liivak O, Calve S, Adaska J, Ji G, Yang Z, et al. Macromolecules 2000;33:775–80.
[19] Zarkoob S, Eby RK, Reneker DH, Hudson SD, Ertley D, Adams WW. Polymer 2004;45:3973–7.
[20] Zhou CZ, Confalonieri F, Medina N, Zivanovic Y, Esnault C, Yang T, et al. Nucleic Acids Res 2000;28:2413–9.
[21] Schmidt-Rohr K, Clauss J, Spiess HW. Macromolecules 1992;25:3273–7.
[22] Holland GP, Lewis RV, Yarger JL. J Am Chem Soc 2004;126:5867–72.
[23] Sambrook J, Frisch EF, Maniatis T. Molecular cloning: a laboratory manual. Cold Spring Harbor, NY: Cold Spring Harbor Press; 1989.
[24] Dicko C, Knight D, Kenney JM, Vollrath F. Int J Biol Macromol 2005;36:215–24.
[25] Ha SW, Asakura T, Kishore R. Biomacromolecules 2006;7:18–23.
[26] Yao J, Ohgo K, Sugino R, Kishore R, Asakura T. Biomacromolecules 2005;5:1763–9.
[27] Tsukada M, Obo M, Kato H, Freddi G, Zanetti F. J Appl Polym Sci 1996;60:1619–27.